Medical Image Analysis 56 (2019) 11–25

Contents lists available at ScienceDirect

Medical Image Analysis

journal homepage: www.elsevier.com/locate/media

Multivariate graph learning for detecting aberrant connectivity of dynamic brain networks in autism

Priya Aggarwal*, Anubha Gupta

Signal processing and Bio-medical Imaging Lab (SBILab), Department of Electronics and Communication Engineering, Indraprastha Institute of Information Technology-Delhi (IIIT-D), Delhi, India

ARTICLE INFO

Article history:
Received 12 August 2018
Revised 1 April 2019
Accepted 24 May 2019
Available online 25 May 2019

Keywords:
Resting-state brain networks
fMRI
Dynamic functional connectivity
Autism
Overlapping networks

ABSTRACT

Alterations in *static* functional brain networks have previously been reported in Autistic Spectrum Disorder (ASD). Although functional brain networks are known to be time-varying, alterations in time-varying or *dynamic* brain networks in ASD is largely unknown. Hence, in this study, we analyze resting-state fMRI data of ASD group versus Typically Developing Control (TDC) group to understand alterations in dynamic functional brain networks in ASD vis-à-vis healthy controls. We introduce a new framework for extracting overlapping dynamic functional brain networks to study these alterations. We utilize sliding window approach along with the recent Multivariate Vector Regression-based Connectivity (MVRC) method to construct functional connectivity (FC) matrices in each time-window. Further, we build three-mode subject-summarized spatio-temporal tensor in both ASD and TDC groups. This tensor is utilized to determine a set of overlapping dynamic functional brain networks and their temporal profiles. This helps us in studying alterations in dynamic brain networks in ASD subjects at the group-level. The proposed framework is tested on two publicly available resting-state fMRI dataset of ASD and normal controls. Our analyses on resting-state fMRI data indicate that dynamic functional brain networks of ASD subjects are altered compared to the TDC group. Two-sample *t*-test is used to establish the statistical significance of the differences observed in network strengths of the two groups. Compared to the TDC subjects, autistic subjects showed alterations in multiple functional brain networks including cognitive control, subcortical, auditory, visual, bilateral limbic, and default mode network. The proposed methodology is able to provide information on alterations in dynamic functional brain networks in ASD and may provide potential biomarkers for studying human brain disorders.

1. Introduction

Autism Spectrum Disorder (ASD) is a neuro-developmental disorder characterized by impairment in social behavior or communication skills and, repetitive behavior or restricted interests (Frith and Happ, 1999). The study of alterations in brain networks and aberrant connectivity in ASD is generally considered a promising approach to find abnormalities in the functioning of human brain (Hull et al., 2017). The connectivity is commonly characterized by (1) structural connectivity that helps to track structural alterations in ASD, (2) effective connectivity that helps to understand the influence of one region over other regions of interest (ROIs), and (3) functional connectivity (FC) that helps to identify functional relationship between pairs of ROIs. Electroencephalograms (EEG), Magnetoencephalograms (MEG), and functional Magnetic Resonance Imaging (fMRI) are functional neuroimaging modalities that are used to study altered FC in ASD subjects. In this study, we utilize fMRI data to study altered functional brain networks because it has higher spatial resolution compared to the other modalities.

In fMRI, a brain volume is scanned multiple times, where each scan consists of a set of images. Strictly speaking, a set of 3D images consisting of multiple voxels (3D volumetric pixel) is acquired. Each voxel's time-series is known as Blood Oxygenation Level-Dependent (BOLD) signal that is an indirect measure of neuronal activity (Ogawa et al., 1990). fMRI has been used for estimating aberrant FC in ASD during a task condition (Minshew and Keller, 2010) and in resting-state condition (Cherkassky et al., 2006). In ASD, BOLD signals have been observed to show aberrant connectivity in many functional networks such as Visual Network (VN), Somato-motor Network (SMN), Auditory Network (AN), Cognitive Control Network (CCN), and Default Mode Network (DMN) (Hull et al., 2017). It is envisaged that the identification of brain networks using FC may provide potential biomarkers to understand the organization and alterations of brain networks in ASD.

* Corresponding author.
E-mail addresses: priyaa@iiitd.ac.in (P. Aggarwal), anubha@iiitd.ac.in (A. Gupta).

https://doi.org/10.1016/j.media.2019.05.007
1361-8415/

Typically, functional brain networks are studied using static functional connectivity (sFC) analysis that assumes networks to be static during the entire scan session. Some studies have shown general impairment in ASD subjects compared with TDC (Hull et al., 2017), some have focused on assessing differences in FC associated with age (Wiggins et al., 2011), and others have focused on alteration of a particular region's connectivity in ASD (Aarti et al., 2014). However, it has been reported that brain networks change with time and are inherently non-stationary over the duration of a single scan (Hutchison et al., 2013b). Hence, sFC may not fully capture these time-varying brain networks. Although dynamic functional connectivity (dFC) based analysis is emerging as a promising technique complementary to sFC (Hutchison et al., 2013b), the study of dFC based fMRI analysis in ASD has been reported only in a few studies (Yao et al., 2016). Yao et al. (2016) studied network states from correlation matrices, but did not extract overlapping dynamic brain networks.

Given that static FC has helped to understand the cognitive impairment in ASD, a dynamic FC approach may add relevant information as it represents the dynamic nature of the brain more accurately. Recent methods in dFC have relied upon sliding window based analysis (Hutchison et al., 2013b). These methods divide the scan into overlapping windows and calculate FC in multiple overlapping time windows. This leads to multiple window-indexed FC matrices. Most work in dFC, until now, focused on identifying non-overlapping communities/networks, where a community is defined as a group of densely interconnected ROIs and is referred to as a functional brain network in our context. This is to note that there is a considerable indication of overlapping brain networks as observed with independent component analysis (Calhoun et al., 2001). Indeed, there is an increasing realization that one brain region may belong to several brain communities/networks simultaneously and thus, overlapping networks may provide critical information about brain's network organization.

FC based overlapping communities have been studied recently for sFC on normal subjects (Najafi et al., 2016; Aggarwal and Gupta, 2018). Although some steps have been taken towards identifying overlapping static communities, literature is still scarce on identifying dynamic communities. To the best of our knowledge, characterization of overlapping dynamic communities in ASD has not been investigated. Overlapping brain networks are important in autism because it is well known that in autism, although brain regions show activation, there is less coordination between regions. This problem leads to reduced attention, difficulty in prioritizing tasks, inhibition in brain required for executing intended tasks, and behavioral problems. All these problems signify that functional brain networks are affected and perhaps, random nodes are grouped together leading to overlapping networks. Hence, this work contributes toward identifying and studying dynamic overlapping networks of both ASD and TDC groups by combining the recently proposed multivariate graph learning method (Aggarwal et al., 2017) and tensor decomposition based processing for identifying overlapping networks. Such a work may add better understanding or aid in the diagnosis of ASD vis-à-vis TDC since the diagnosis of ASD is quite challenging owing to it being a disorder over wider spectrum (varying degree of autism across subjects and hence, is called autism spectral disorder or ASD).

Key contributions of this work are as follows:

- A tensor-based model for the identification of multi-subjects' dynamic functional brain networks is proposed.
- A framework is developed for the discovery of overlapping functional brain networks using tensor factorization.
- The performance of the proposed method is evaluated on two publicly available fMRI dataset consisting of ASD and TDC subjects. Consistent findings, illustrating differences between ASD versus TDC groups, has been observed in all tests.

The remainder of this paper is organized as follows. We present data description with the methodology in Section 2, experimental results in Section 3, results in Section 4 followed by concluding remarks in Section 5.

2. Materials and methods

2.1. Data description

In this study, we have used two publicy available dataset that are described below.

Dataset-1 (GU dataset): This is the publicly available Autism dataset contributed by Georgetown University at the collection site of Autism Brain Image Data Exchange II (ABIDE II[1]). This dataset includes echo-planar images acquired on a Siemens Trio 3-T scanner using an Echo Time (TE) equal to 30 ms and Repetition Time (TR) equal to 2000 ms. It includes fMRI data of 55 TDC (age: 8.1 - 13.8 years) and 51 ASD subjects (age: 8.1 - 13.9 years) scanned during the resting state. Subjects underwent a 5 min, 14 s resting state scan with their eyes open in the awaken state. The fMRI data is collected for 152 brain volumes with 43 axial brain slices (dimension 64×64) in each volume.

Dataset-2 (KKI dataset): This dataset is the pediatric Autism datasest contributed by Kennedy Krieger Institute (KKI) at the collection site of ABIDE II. This dataset is chosen due to similar age subjects as that with GU dataset. This dataset consists of 155 TDC (age: 8 - 13 years) and 56 ASD subjects (age: 8 - 13 years). Images are acquired on a Philips 3-T scanner using an Echo Time (TE) equal to 30 ms and Repetition Time (TR) equal to 2500 ms. Subjects underwent a 6 min, 40 s resting state scan with fMRI data collected with 47 axial brain slices (dimension 64×64) in each volume.

2.2. Data preprocessing

All BOLD images are pre-processed using SPM12 (Statistical Parametric Mapping[2]). First five brain volumes, accounting for T1 equilibration effect, are discarded in both dataset. The other functional volumes are slice time corrected, motion corrected, spatially normalized onto the Montreal Neurological Institute (MNI) space resulting into functional images of dimension $53 \times 63 \times 52$ (3-mm isotropic voxels) that are smoothed with a Gaussian kernel of 6 mm full width half maximum. Finally, nuisance variables (6 head motion parameters, average cerebro-spinal fluid signal from ventricular mask, and average white matter signal from white matter mask) are regressed out from each voxel's time series followed by bandpass filtering in the frequency range of 0.01 to 0.08 Hz.

Framewise displacement (FD) is used to identify temporal artifact in each subject by calculating the derivatives of the six rigid-body realignment parameters estimated during motion correction preprocessing step (Power et al., 2014). Subjects having more than 30% of total brain volumes with $FD > 0.5$mm were excluded from further analysis. This led to the rejection of 4 out of 55 TDC subjects' data and 12 out of 51 ASD subjects' data from dataset-1, and rejection of 14 out of 99 TDC subjects' data and 2 out of 41 ASD subjects' data from dataset-2. This is to note that head motion was minimized in dataset-1 by placing foam cushions in the space between the participant's head and the headcoil. We included only male subjects in both the dataset to control for

[1] http://fcon_1000.projects.nitrc.org/indi/abide/.
[2] http://www.fil.ion.ucl.ac.uk/spm/software/spm12/.

Table 1
Summary of TDC versus ASD Subjects' data.

	Dataset-1	(GU)	Dataset-2	(KKI)
Characteristic	TDC (S=26)	ASD (S=35)	TDC (S=85)	ASD (S=39)
Gender	Male	Male	Male	Male
Age (years)				
Mean (SD)	10.9 (1.62)	11.17 (1.49)	10.44 (1.49)	10.49 (1.53)
Range	8.06–13.79	8.25–13.91	8.02–13	8.01–12.99
Full Scale IQ				
Mean (SD)	120.32 (13.53)	119.06$^{\gamma}$ (14.18)	114.9 (11.04)	101.8$^{\gamma}$ (15.93)
Range	91–148	95–149	94–140	84–148
ADI-R				
Social total A	–	19.74$^{\gamma}$ (5.28)	–	20.29 (4.08)
Verbal total BV	–	14.97$^{\gamma}$ (4.91)	–	15.75 (3.15)
RRB total C	–	5.09$^{\gamma}$ (2.38)	–	8.41 (2.45)
R Onset total D	–	2.56$^{\gamma}$ (1.23)	–	6.07 (2.03)
ADOS				
Total	–	10.52$^{\Upsilon}$ (4.61)	–	–
Communication	–	3.18$^{\Upsilon}$(1.54)	–	–
Social	–	7.33$^{\Upsilon}$ (3.53)	–	–
Stereo Behavior	–	1.89$^{\Upsilon}$ (1.58)	–	–

$^{\gamma}$One subject's score is missing. $^{\Upsilon}$Seven ASD subjects do not have these scores. ' - ' signifies that these scores are not available for the TDC group. TDC: Typically Developing Control; ASD: Autism Spectrum Disorder; ADI-R: Autism Diagnostic Interview-Revised; Social total A: Reciprocal Social Interaction Subscore A; Verbal total BV: Abnormalities in Verbal Communication Subscore; RRB total C: Restricted, Repetitive, and Stereotyped Patterns of Behavior; ADOS: Autism Diagnostic Observation; Stereo Behavior: Stereotyped Behaviors and Restricted Interest.

Table 2
List of indices and regions in the AAL 90 template.

Index	Region	Index	Region
(1,2)	Precental gyrus (PG)	(47,48)	Lingual gyrus (LG)
(3,4)	Superior frontal gyrus, dorsolateral (DSFG)	(49,50)	Superior occipital gyrus (SOG)
(5,6)	Superior frontal gyrus, orbital part (OSFG)	(51,52)	Middle occipital gyrus (MOG)
(7,8)	Middle frontal gyrus (MFG)	(53,54)	Inferior occipital gyrus (IOG)
(9,10)	Middle frontal gyrus, orbital part (OMFG)	(55,56)	Fusiform gyrus (FG)
(11,12)	Inferior frontal gyrus, opercular part (OPIFG)	(57,58)	Postcentral gyrus (POG)
(13,14)	Inferior frontal gyrus, triangular part (TIFG)	(59,60)	Superior parietal gyrus (SPG)
(15,16)	Inferior frontal gyrus, orbital part (OIFG)	(61,62)	Inferior parietal, but supramarginal and angular gyri (SMAG)
(17,18)	Rolandic operculum (RO)	(63,64)	Supramarginal gyrus (SMG)
(19,20)	Supplementary motor area (SMA)	(65,66)	Angular gyrus (AG)
(21,22)	Olfactory cortex (OC)	(67,68)	Precuneus (PRE)
(23,24)	Superior frontal gyrus, medial (MSFG)	(69,70)	Paracentral lobule (PL)
(25,26)	Superior frontal gyrus, medial orbital (MOSFG)	(71,72)	Caudate nucleus (CN)
(27,28)	Gyrus rectus (GR)	(73,74)	Lenticular nucleus, putamen (PUT)
(29,30)	Insula (INS)	(75,76)	Lenticular nucleus, pallidum (PAL)
(31,32)	Anterior cingulate and paracingulate gyri (ACC)	(77,78)	Thalamus (THA)
(33,34)	Median cingulate and paracingulate gyri (MCPG)	(79,80)	Heschl gyrus (HG)
(35,36)	Posterior cingulate gyrus (PCC)	(81,82)	Superior temporal gyrus (STG)
(37,38)	Hippocampus (HIP)	(83,84)	Temporal pole: superior temporal gyrus (TSTG)
(39,40)	Parahippocampal gyrus (PHG)	(85,86)	Middle temporal gyrus (MTG)
(41,42)	Amygdala (AMY)	(87,88)	Temporal pole: middle temporal gyrus (TSTG)
(43,44)	Calcarine fissure and surrounding cortex2 (CF)	(89,90)	Inferior temporal gyrus (ITG)
(45,46)	Cuneus (CUN)		

The odd and even indices represent left (L) and right (R) brain hemisphere regions, respectively.

gender differences that may be associated with functional brain networks. After quality check, a total of 26 TDC and 35 ASD subjects remained from Dataset-1 (GU) and a total of 85 TDC and 39 ASD subjects remained from Dataset-2 (KKI) for our analysis. A two-sample t-test with unequal variance showed no significant difference (at $p < 0.05$ significance level) in the age of two groups of both the dataset (Table 1).

Preprocessed data is parcellated into 90 anatomical predefined ROIs via Automated Anatomical Labeling (AAL) atlas (refer to Table 2) (Tzourio-Mazoyer et al., 2002). We averaged the time-series of all voxels belonging to the same ROI to find the region-representative time series of every ROI. This resulted into a matrix $\mathbf{X}$ of dimension $T \times N$, where T denotes the number of time points and N=90 denotes the number of ROIs obtained with AAL atlas. Network labels corresponding to each of the 90 ROIs are listed at the bottom of Table 2, based on the information provided in (Karahanolu et al., 2013).

2.3. Multivariate vector regression-based static connectivity

FC in individual participant is identified using the recently proposed MVRC method (Aggarwal et al., 2017). For the sake of completeness, we first review the MVRC method of finding sFC (Aggarwal et al., 2017). This method regresses the time-series of all regions (columns of $\mathbf{X}$) onto the time-series of other regions and estimates the adjacency matrix with the elastic-net penalty as shown below:

$$\min_{\tilde{\mathbf{W}}} \frac{1}{2}\left\|\mathbf{X} - \mathbf{X}\tilde{\mathbf{W}}\right\|_F^2 + \mu_1\left\|\tilde{\mathbf{W}}\right\|_1 + \mu_2\left\|\tilde{\mathbf{W}}\right\|_F^2 \quad (1)$$

where μ_1 and μ_2 are the regularization parameters and $\mathbf{X} \in \mathbb{R}^{T\times N}$ contains the time-series of all N brain regions with T number of time points. Since matrix $\tilde{\mathbf{W}}$ is not symmetric, a positive symmetric adjacency or FC matrix $\mathbf{G}$ is obtained by $\mathbf{G} = (\left|\tilde{\mathbf{W}}\right| + \left|\tilde{\mathbf{W}}\right|^T)/2$. For

more details on MVRC method and its implementation, one may refer to Aggarwal et al. (2017).

2.4. Learning multivariate regression-based dynamic connectivity

This is to note that MVRC method utilizes data of all T time points in (1) to build the FC matrix $\mathbf{G}$ and hence, leads to the extraction of static functional brain networks (Aggarwal et al., 2017). However, brain networks are known to be dynamic, wherein network connections and their strengths change with time. One of the most common ways to identify dFC is the sliding window approach, where a temporal window of a certain time duration is decided and slided by one time point, in general, to capture dynamic brain networks. This process is repeated until all T time points are covered via sliding windows. Inside each single window, FC is estimated independently of the data of other windows and networks are assumed to be static within the duration of each window length. In this paper, we have utilized MVRC method (Aggarwal et al., 2017) in every window to estimate the FC matrix $\mathbf{G}_w \in \mathbb{R}^{N\times N}$, where the subscript w denotes the w^{th} window. We computed this matrix in each time-window and formed a tensor $\mathcal{T}$ of dimension $N\times N\times L$, where N denotes the number of ROIs and L denotes the total number of windows. dFC requires predefined window length in sliding window approach. There is always a dilemma in choosing an appropriate window length because results are strongly dependent on the chosen window length (Hutchison et al., 2013b). Shorter windows may provide spurious changes in dFC leading to difficulties in distinguishing signals of interest from other confounding factors (Chang and Glover, 2010). On the other hand, larger duration windows may not capture time-varying functional networks. In a recent work, it has been shown that window length is dependent on the preprocessing step of bandpass filtering of BOLD time series (Leonardi and Ville, 2015). Lowest frequency $f_{\min}$ of the filter provides an appropriate window length that is equal to $1/f_{\min}$ (Leonardi and Ville, 2015). It is a simplified relationship between the window length and the frequency content of a signal. We utilized this approach to select the window duration. We considered a window length of 100 s corresponding to the lowest frequency of 0.01Hz used in our pre-processing step of filtering. With TR=2 s of the Autism dataset, this corresponds to 50 time points in one window (50 TR). This window length helps us in capturing one full cycle of the slowest bandpass filtered frequency component.

2.5. Group-level summarized dFC

For every subject of a group, we computed tensors $\mathcal{T}$ with dimension $N\times N\times L$ (region $\times$ region $\times$ window). We carry out group-level dFC summarization that helps us in comparing TDC versus ASD group-level differences/alterations in dynamic brain networks.

Generally, adjacency matrices are averaged over subjects to form a single group-averaged adjacency matrix (Thompson and Fransson, 2015; Robinson et al., 2015). Since this averaging considers equal contribution of every subject's data to the resultant adjacency matrix, it would result in loss of inter-subject variability. Hence, in this work, we identified subject-summarized adjacency matrix in each time-window by estimating activation associated with each subject.

We used dFC matrices of all subjects (region $\times$ region $\times$ subject) in one time-window w to identify group-level FC matrix (with dimension region $\times$ region). The collection of adjacency matrices of all subjects $s = 1, 2, \ldots, S$ in one time-window forms a three-mode spatio-subject tensor $\mathcal{X} \in \mathbb{R}^{N\times N\times S}$, where N denotes the number of ROIs and S denotes the total number of subjects. The value of S may differ in the TDC and ASD groups.

We utilized Tucker decomposition of $\mathcal{X} \in \mathbb{R}^{N\times N\times S}$ (Lathauwer et al., 2000), to obtain $N\times N$ adjacency matrix in one time-window. It computes orthonormal subspaces corresponding to each mode of the tensor and is defined as below:

$$\mathcal{X} = \mathcal{C} \times_1 \mathbf{U}_1 \times_2 \mathbf{U}_2 \times_3 \mathbf{U}_3, \tag{2}$$

where $\mathcal{C} \in \mathbb{R}^{N\times N\times S}$ is the core tensor, $\times_k$ represent mode k product, and $\mathbf{U}_1 \in \mathbb{R}^{N\times N}$, $\mathbf{U}_2 \in \mathbb{R}^{N\times N}$ and $\mathbf{U}_3 \in \mathbb{R}^{S\times S}$ denote the orthonormal mode matrices along all the three modes. The columns of $\mathbf{U}_3$ provide connectivity information about subjects. The first left vector ($\mathbf{u}_{3,1} \in \mathbb{R}^{S\times 1}$) of matrix $\mathbf{U}_3$ represents the most significant vector capturing highest functional connectivity energy of subjects in time-window w (Mahyari et al., 2017; Zhang et al., 2015). Hence, we utilized $\mathbf{u}_{3,1}$ to obtain the subject-summarized adjacency matrix $\mathbf{D}(w) \in \mathbb{R}^{N\times N}$ of time-window w as:

$$\mathbf{D}(w) = \frac{\sum_{s=1}^{S} \mathbf{u}_{3,1}(s)\mathbf{G}_w(s)}{\sum_{s=1}^{S} \mathbf{u}_{3,1}(s)}, \tag{3}$$

where $\mathbf{G}_w(s)$ is the MVRC adjacency matrix of subject s in the wth time-window. Similar processing in all L windows results in a three-mode spatio-temporal tensor $\mathcal{T}$ of dimension $N\times N\times L$ (region x region x window), summarized over all subjects as mentioned above.

2.6. Extracting dynamic networks

Next, we partitioned these estimated whole-brain dFC into non-overlapping and overlapping networks as explained below. Each network contains several densely interconnected regions, while there are relatively few connections between regions belonging to different networks.

2.6.1. Determination of non-overlapping networks by modularity

Previous works on extracting networks from dFC matrices are largely based on the computation of modularity. These methods provide non-overlapping networks, i.e., each region belongs to only one network. These networks are identified by maximizing the quality function Q of modularity (Newman and Girvan, 2004). The quality function Q is defined as:

$$Q_{uni} = \sum_{i,\ j} [G_{ij} - \gamma P_{ij}]\delta(c_i, c_j), \tag{4}$$

where G_{ij} denotes the (i, j)th entry of the weighted adjacency matrix $\mathbf{G}$, δ represents Kronecker delta with $\delta(c_i, c_j) = 1$ if $c_i = c_j$ and 0 otherwise, c_i denotes the ith region belonging to network c, γ is a resolution parameter generally set to 1 because $\gamma > 1$ leads to detection of smaller modules and $0 \le \gamma < 1$ leads to detection of larger modules (Rubinov and Sporns, 2010). P_{ij} denotes the expected weight on edge connecting region i and region j under the Newman–Girvan null model and is defined as (Newman and Girvan, 2004):

$$P_{ij} = \frac{k_i k_j}{2\sum_{i,\ j} G_{ij}} \tag{5}$$

where k_i and k_j are the degrees of regions i and j, respectively. A high value of Q is desirable for identifying the most optimal network structure. Modularity is computed separately on each connectivity matrix $\mathbf{G}_w$ within each time-window.

We used Newman community/network detection algorithm to optimize modularity (Newman, 2006). Due to the stochastic nature of this algorithm, we repeated the estimation 100 times to get a consensus partition. We computed the modular (binary) allegiance matrix for each of the 100 runs, whose (ij)th element implies whether regions i and j are assigned to the same network or not. Combined consensus matrix is obtained by averaging

all the modular allegiance matrices. Modularity is again applied on the consensus matrix to obtain the final consensus networks (Sporns and Betzel, 2016).

Next, we calculated the within-module degree z-score and the participation coefficient (PC) for each brain network (Guimera and Nunes Amaral, 2005). Module degree z-score describes the within-module connectivity strength, whereas PC describes the connectedness of regions across different modules. For region i, within-module degree is defined as:

$$z_i = \frac{k_i - < k_i >}{\sigma_{k_i}}, \tag{6}$$

where k_i denotes the degree of region i in a network, $< k_i >$ denotes the average degree of all the regions in the same network, and σ_{k_i} denotes the standard deviation of all regions' degrees.

PC describes the extent to which a region belonging to one network c is connected to regions of other networks. It is defined as:

$$P_i = 1 - \sum_c (\frac{k_{ic}}{k_i})^2, \tag{7}$$

where k_{ic} denotes the number of connections between region i and other regions within network c and k_i denotes the degree of region i. A threshold of mean plus one standard deviation of z-values are considered for identifying "connector" hubs in each time-window, while a threshold of mean plus one standard deviation of PC are considered for identifying "provincial" hubs in each time-window. Regions with values higher than the threshold and reproducible with 90% or higher percentile in all time windows are considered "connector" hubs for the case of module-degree z-score and "provincial" hubs for the case of PC.

2.6.2. Identifying overlapping networks

A dFC is partitioned into non-overlapping networks using modularity, i.e., each region belongs to one network only. Since certain brain regions may be involved in more than one network, it suggests for the identification of overlapping networks (Najafi et al., 2016). There are various algorithms that estimate overlapping networks, such as mixed membership algorithm proposed in Najafi et al. (2016) and non-negative tensor factorization (NNTF) proposed in Ponce-Alvarez et al. (2015). In this work, we utilized NNTF to extract overlapping networks. To the best of our knowledge, this is the first study that compares overlapping networks in a neuro-development disorder.

We performed Parallel Factor (PARAFAC) decomposition (Kolda and Bader, 2009) of dFC tensor $\mathcal{T}$ as estimated in Section 2.4. Given a rank R, it decomposes input tensor $\mathcal{T}$ into a sum of R number of rank-one tensors, generated by the outer product of column vectors as below:

$$\mathcal{T} \approx \sum_{r=1}^{R} \lambda_r \boldsymbol{a}_r \circ \mathbf{b}_r \circ \mathbf{c}_r, \tag{8}$$

where '$\circ$' denotes the outer product, $\boldsymbol{a}_r \in \mathbb{R}^{N\times 1}$, $\mathbf{b}_r \in \mathbb{R}^{N\times 1}$, and $\mathbf{c}_r \in \mathbb{R}^{L\times 1}$ denote the loading vectors corresponding to each mode of tensor $\mathcal{T}$ and R denotes the number of rank-one tensors (also called as the number of components). The decomposition in (8) is expressed in the matrix form as:

$$\mathcal{T} \approx \mathcal{D} \times_1 \mathbf{A}_R \times_2 \mathbf{B}_R \times_3 \mathbf{C}_R, \tag{9}$$

where $\mathcal{D}$ is the diagonal core tensor and $\mathbf{A}_R = [\boldsymbol{a}_1, \ldots, \boldsymbol{a}_R] \in \mathbb{R}^{N\times R}$, $\mathbf{B}_R = [\mathbf{b}_1, \ldots, \mathbf{b}_R] \in \mathbb{R}^{N\times R}$, and $\mathbf{C}_R = [\mathbf{c}_1, \ldots, \mathbf{c}_R] \in \mathbb{R}^{L\times R}$ are the component matrices containing R loading vectors. $\times_{(.)}$ denotes the tensor product. This is to note that the column dimension of each of the component matrix is R in the PARAFAC model in (9). Here, components one and two provide loading vectors corresponding to regions and component three provides temporal loading vector. Since the adjacency matrix is symmetric in the first two modes of the tensor $\mathcal{T}$, components one and two are similar.

Modes one and two of tensor $\mathcal{T}$ contain the connectivity matrices with non-negative values. Hence, we add non-negative constraint on all components $\mathbf{A}_R$, $\mathbf{B}_R$, and $\mathbf{C}_R$ in (9). Similarly, as aforementioned, matrices $\mathbf{A}_R$ and $\mathbf{B}_R$ are identical because the adjacency matrix is symmetric. There are many algorithms for carrying out non-negative PARAFAC decomposition. We applied the block principal pivoting algorithm[3] because of its good performance in fMRI studies (Ponce-Alvarez et al., 2015). Further, we utilized the core consistency method for determining R values for both TDC and ASD groups (Gauvin et al., 2014). One may refer to Gauvin et al. (2014) for further details of this method.

Identifying networks from loading vectors: We utilized each column of $\mathbf{A}_R$ component matrix to identify R number of networks. Loading vectors $\boldsymbol{a}_r$ or $\mathbf{b}_r$, for $r = 1, 2, \cdots, R$, provide the membership of regions to the component or network r, whereas $\mathbf{c}_r$ provides their time-varying or the temporal profile. A high value of ith element of loading vector $\boldsymbol{a}_r$ represents greater membership of the corresponding ith region to that component r. Hence, thresholding on loading vectors $\boldsymbol{a}_r$ would capture networks as collection of ROI with higher membership. Fig. 1 depicts a few loading vectors $\boldsymbol{a}_r$ and $\mathbf{c}_r$ for both TDC and ASD groups considering R=10. Fig. 1 shows two randomly selected loading vectors of both TDC (Fig. 1A) and ASD (Fig. 1B) groups. ROI loading vectors $\boldsymbol{a}_r$ represent membership values of 1 to N ROI. Similarly, temporal loading vectors $\mathbf{c}_r$ represent time varying profiles.

From Fig. 1, we observe that every loading vector $\boldsymbol{a}_r$ has a few regions with higher membership values and rest with very less values in both TDC and ASD groups. Hence, we carry out thresholding of these vectors that results in networks of ROI. We considered mean plus one standard deviation as the threshold on each loading vector. Regions with membership values exceeding the above specified threshold in vector $\boldsymbol{a}_r$ are considered a part of the rth network. This leads to the detection of overlapping networks. This is essential because one region can be a part of multiple networks owing to the relationship between different networks. For example, an auditory stimulus may trigger recollection of past events. In such a case, auditory and cognitive control networks may have some connected/overlapping regions. *Strength of networks:* Further, strength of each network is computed from it's ROI loading vector and temporal loading vector as $\mathbf{s}_r = \mathbf{c}_r \sum_i \boldsymbol{a}_r(i)$. This formulation was first proposed to compute the strength of communities in social networks (Gauvin et al., 2014). We utilized strength vectors of similar networks in TDC and ASD groups to identify altered functional brain networks.

Fig. 2 shows the complete process of extracting dynamic functional brain networks.

2.7. Statistical analysis

We have done a thorough statistical analysis of dynamic networks. We looked at both overlapping and non-overlapping networks. For overlapping networks, we tested for statistically significant differences in similar networks, identified using strength of networks of TDC and ASD groups. Further, for subject-summarized dynamic connectivity, we investigated statistical differences between modularity quality function. Given 90 ROIs, we also assessed differences between connector and provincial non-overlapping hubs extracted using modularity. Results were considered statistically significant for a value of $p < 0.05$. We used two-sample t-test

[3] www.cc.gatech.edu/~hpark/nmfsoftware.php.

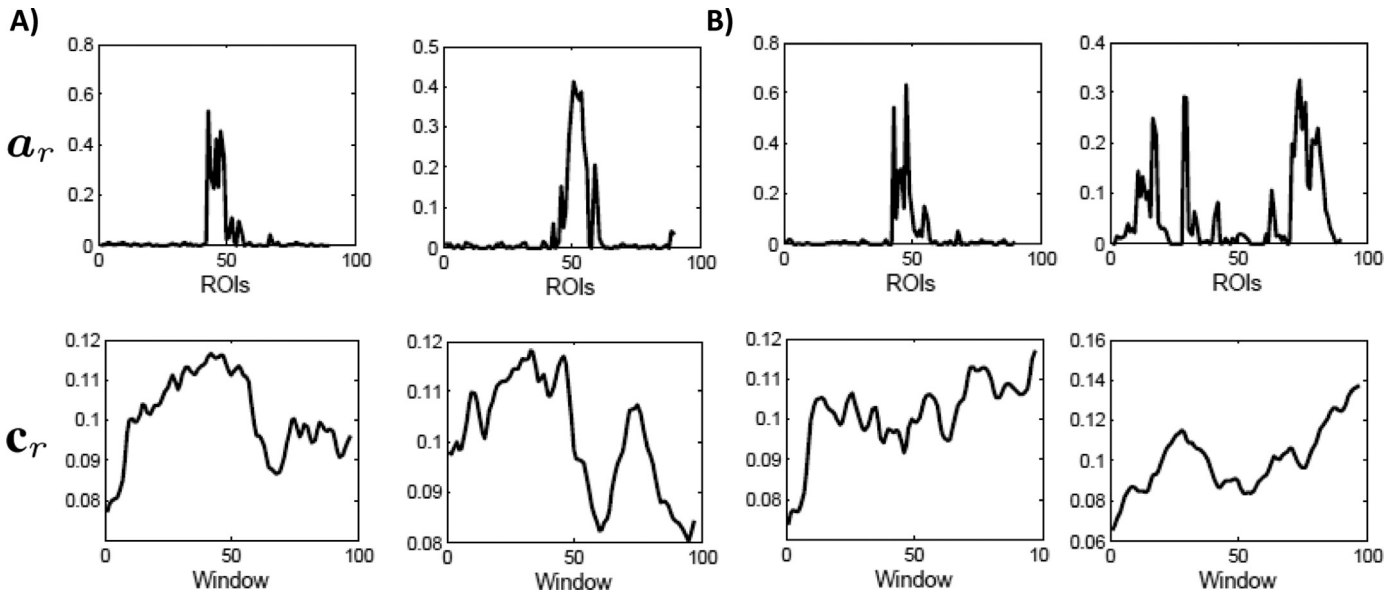

Fig. 1. Results on GU dataset: We present two randomly selected loading vectors, obtained with R=10, for both (A) TDC and (B) ASD groups. Vector $\boldsymbol{a}_r$ represents ROI loading vectors containing membership values of each region to the rth network and $\mathbf{c}_r$ presents information about the temporal loading vector corresponding to the rth network.

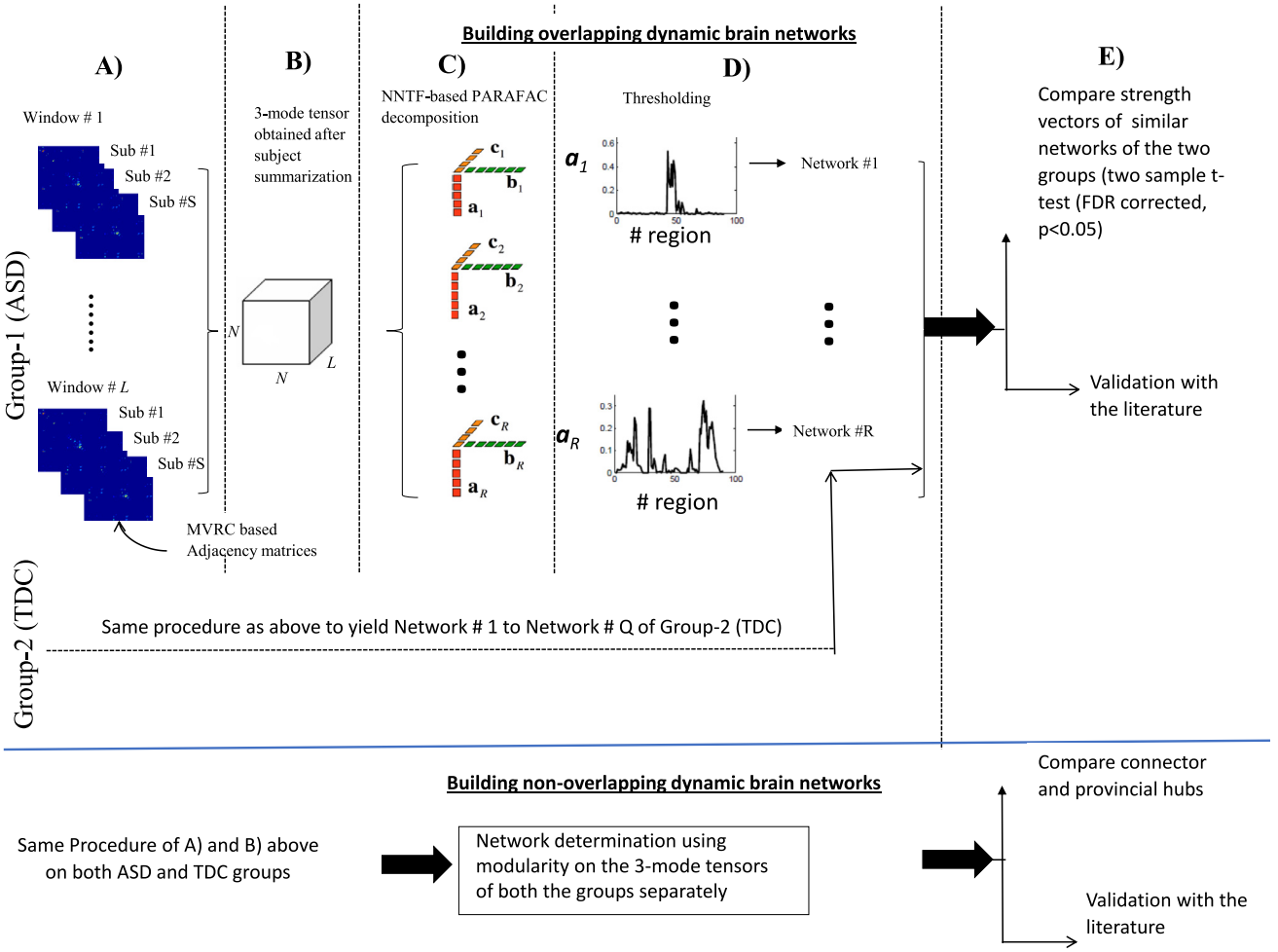

Fig. 2. Determination of overlapping and non-overlapping dynamic functional brain networks (A) MVRC based adjacency matrices are computed for all subjects in each time-window for both the groups, (B) 3-mode tensor of size $N \times N \times L$ is obtained after subject summarization in both the groups; top half (C) Non-negative tensor factorization (NNTF) based PARAFAC decomposition with R factors where the first and second components represent region loading vectors, and the third component represents the time loading vector. (D) overlapping networks are obtained by thresholding each region's loading vectors. bottom half Non-overlapping network determination of both the groups using modularity, (E) Validation of results.

for testing the statistical significance of differences between two groups. We also corrected for multiple comparison using false discovery rate (FDR) (Benjamini and Hochberg, 1995) with $p < 0.05$, whereever needed.

3. Results

Our primary interest is to report disease-driven changes in functional brain networks. We computed dFC matrices using MVRC. Further, we studied both overlapping and non-overlapping dynamic functional brain networks. We would like to examine if the proposed approach can report changes in FC induced by ASD via comparing the results with the TDC group. First, we present results on GU dataset. We will use KKI dataset to demonstrate the reproducibility of results in Section 3.5.

3.1. Non-Overlapping dynamic functional brain networks identified using modularity

To have a better understanding of dFC states, we estimated modularity based networks that play a pivotal role in the organization of overall networks. We estimated non-overlapping networks using modularity from tensor $\mathcal{T}$, as explained in the previous section, in both TDC and ASD groups. We could identify 3 to 6 number of networks across all time windows in the TDC group. The number of networks for ASD group was 4 to 6. With less number of detected networks, regions belonging to multiple functional brain networks were found to club randomly. With 6 numbers of detected networks in both TDC and ASD groups, we could locate the following functional networks: network 1- SMN, AN; network 2- BLN, DMN; network 3- CCN, LN; network 4- BLN, SCN; network 5- VN; network 6- DMN.

The value of the modularity quality function Q is ranged between 0.5479 to 0.7821 for the TDC and between 0.6038 to 0.7720 for the ASD group. Significant differences were observed in the Q values of both the groups ($p < 0.05$, two sample t-test) that indicates that the quality of partitioning of dynamic functional brain networks using modularity is distinguishable across the two groups, although we did not observe consistency in networks of all time windows as mentioned above. In addition, we observed random grouping of regions in networks. At times, modularity is assessed on the FC matrix averaged across all time windows. However, this procedure results in loss of temporal characteristics associated with dynamic networks and hence, we did not employ averaging on adjacency matrix for our analyses.

To have further understanding of the hubs' architecture in dFC networks, we estimated the connector and provincial hubs' architecture using the module-degree and the PC, respectively. Higher module-degree connector hubs in the TDC group was shown by nine regions: bilateral rolandic operculum, bilateral medial superior frontal gyrus, bilateral medial orbital superior frontal gyrus, left superior occipital gyrus, and bilateral putamen. In the ASD group, connector hubs were formed by nine regions: left dorsolateral superior frontal gyrus, left rolandic operculum, left medial superior frontal gyrus, right anterior cingulate cortex, right parahippocampal gyrus, left superior occipital gyrus, left postcentral gyrus, right precuneus, and right putamen. Among these regions, four common regions (left rolandic operculum, left medial superior frontal gyrus, left superior occipital gyrus, right putamen) were located in the hubs of both ASD and TDC groups and regions such as left dorsolateral superior frontal gyrus, right anterior cingulate cortex, right parahippocampal gyrus, left postcentral gyrus, and right precuneus were located as connector hubs in the ASD group.

Regions showing higher PC in both the TDC and ASD groups comprise left parahippocampal gyrus, right amygdala, bilateral supramarginal gyrus, left angular gyrus, bilateral temporal pole superior temporal gyrus, and bilateral inferior temporal gyrus. This suggests of no alterations in the provincial hubs across the two groups.

3.2. Overlapping dynamic functional brain networks identified using PARAFAC decomposition

As presented in (8), the spatio-temporal tensor $\mathcal{T}$ is decomposed into R number of rank-one tensors, where R represents the number of networks. The value of R is decided according to the core consistency (Gauvin et al., 2014). We considered initial value of R from 2 to 15. For each value of R, we computed the core consistency value and the plot of these values as a function of R is shown in Fig. 5. From this figure, we observe an abrupt change in slope at R=10 for both TDC and ASD groups, where the value of core consistency is more than 0.5. Since core consistency value of above 0.5 is considered acceptable (Gauvin et al., 2014) and the corresponding range of R is considered to be the optimal range, we considered $R = 10$ for both the groups.

After estimating the value of R, we factorized tensor $\mathcal{T}$ into R components. We identified ten overlapping dFC networks in both TDC and ASD groups as shown in Fig. 3 and Fig. 4, respectively. From these figures, we note that the spatio-subject tensor decomposition results in multiple functional brain networks in both TDC and ASD groups. We could identify Visual Network (VN), Auditory Network (AN), Bilateral Limbic Network (BLN), Default Mode Network (DMN), Somato-Motor Network (SMN), Subcortical Network (SN), Language Network (LN), and Cognitive Control Network (CCN).

In order to quantitatively justify the advantage of overlapping brain networks, it is important to first explore nodes that are present in multiple networks indicating overlap between brain networks. From Fig. 8, we observe that the nodes of visual network are present in multiple networks of the normal group. The presence of this network in multiple communities should be justifiable by higher degree or strength (for the case of weighted FC) compared to other networks' nodes because these are the nodes connecting multiple communities and hence, must have a higher number of first order connections. Based on this intuition, we computed the strength of each node in every time-window in the normal group. Further, nodes with strength values higher that 90th percentile in each time-window are grouped together to quantify overlapping nodes. Fig. 6 depicts the histogram of higher strength-valued nodes across all time windows. This figure indicates larger strength of visual nodes (number 43 to 56) compared to other nodes indicating the presence of these nodes in multiple communities and hence, validates the overlap of visual networks with other functional networks. This helped us quantify the presence of overlapping communities in brain networks. Thus, extraction of non-overlapping brain networks may lead to incomplete/incorrect findings about brain regions' participation in multiple networks and may lead to wrong inferences compared to when overlapping communities are considered.

Averaging about subjects may lead to incorrect results because every subject may have different connectivity and excitation. Ideally, this variability should be captured appropriately instead of simply averaging about subjects. Hence, intuitively, averaging may lead to incomprehensible results compared to the proposed subject-summarization method. In order to verify this, we plot the histogram of high strength nodes for the subject-averaged case in Fig. 7. We observe the histogram to be more or less evenly distributed across the number of nodes. This corresponds to hugely overlapping networks with many nodes having higher strength. This shows that clear networks could not be identified with the subject-averaged method.

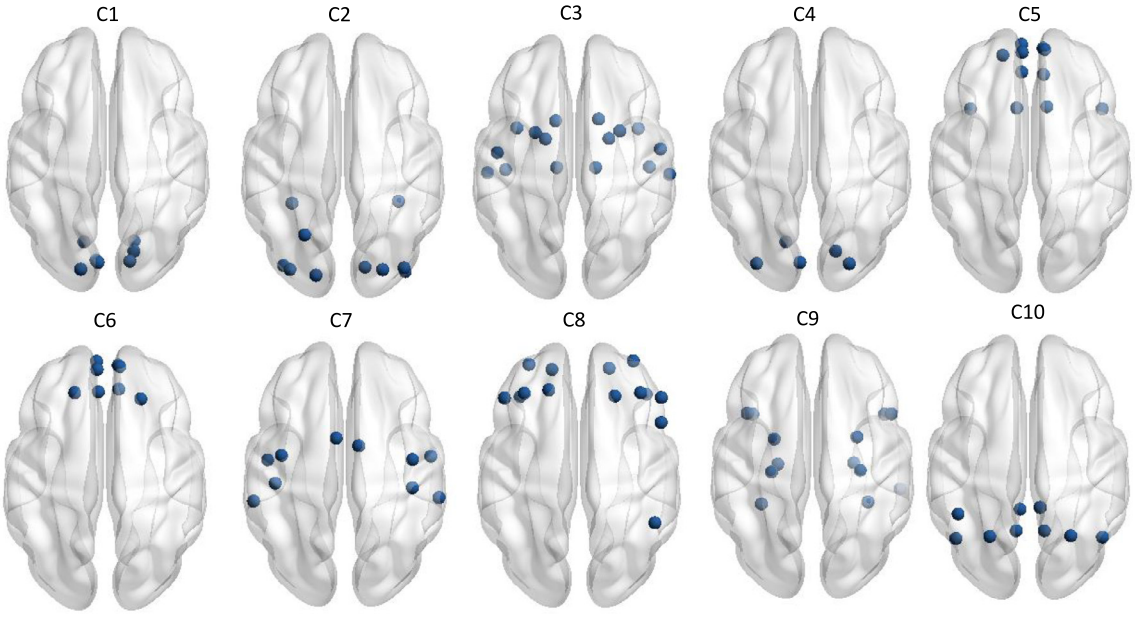

Fig. 3. Group-level dFC networks (denoted as community 1 (C1) to community 10 (C10) identified on TDC subjects of GU dataset.

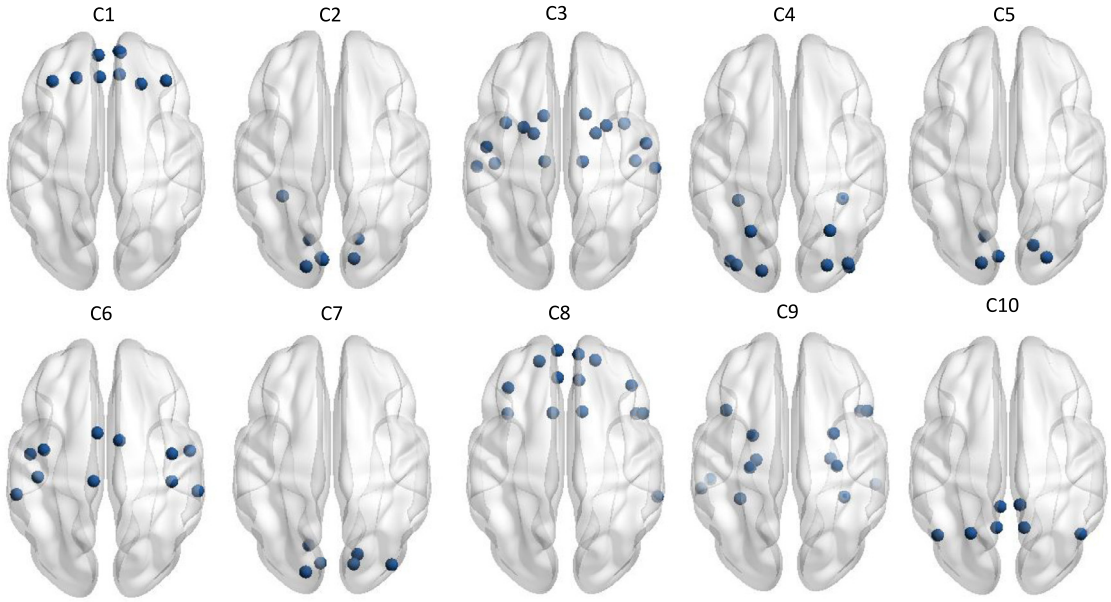

Fig. 4. Group-level dFC networks (denoted as community 1 (C1) to community 10 (C10) identified on ASD subjects of GU dataset.

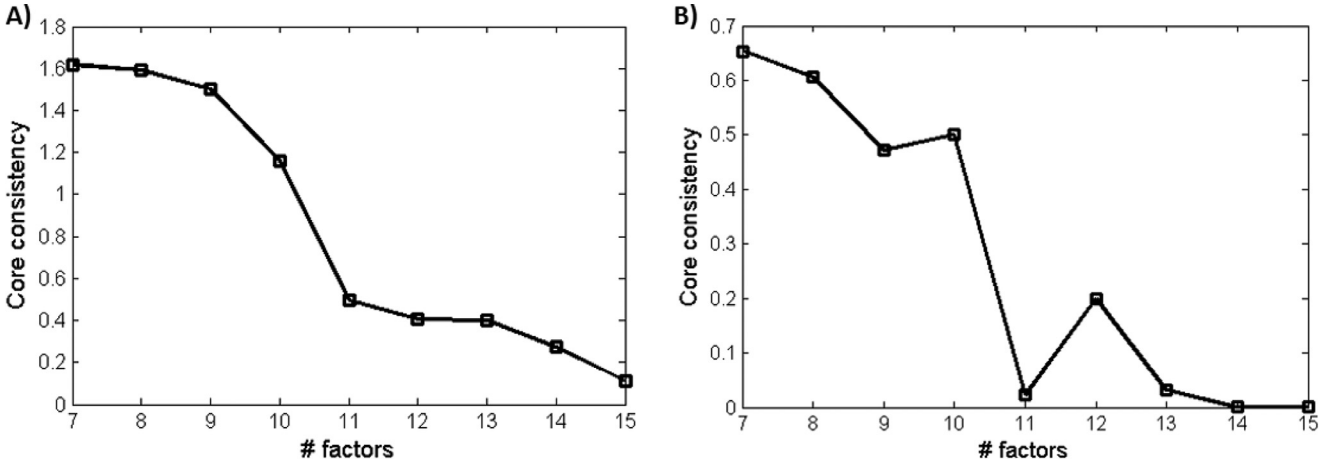

Fig. 5. Plot of core consistency with varying number of components in A) TDC and B) ASD groups of GU dataset.

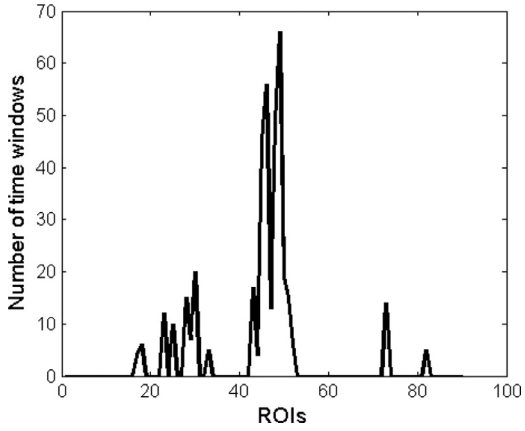

Fig. 6. Histogram of nodes with high-strength computed in all time windows in TDC group, where y-axis denotes the number of time windows in which a node is found to be present with higher strength.

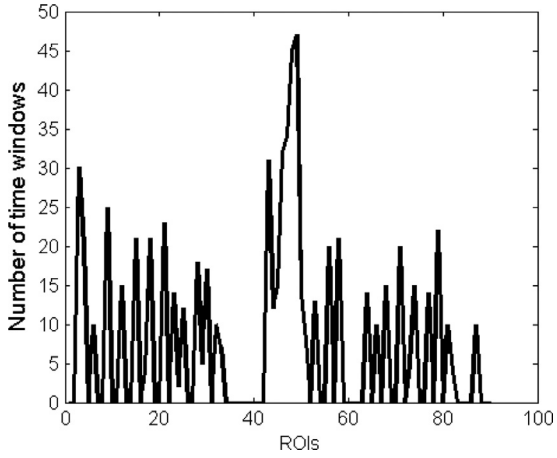

Fig. 7. Frequency of nodes with higher strength (number of time windows in which the strength of a node is high) computed with subject-averaged dFC in TDC group.

Comparison of Networks in ASD and TDC Groups

To compare the strength of identified dFC networks among both the groups, we compared the strength of similar networks. Similar networks are defined as subset of connected network nodes forming distinct brain networks such as auditory network, visual network etc. For example, nodes 43 to 56, presented in Table 2 are associated with visual network. Thus, any network in both the groups (i.e. normal or disease) having most of these nodes can be said to be similar networks (visual networks). We computed the strength vectors $\mathbf{s}_r$ (see Section 2.6) of similar networks in both the groups and examined the statistically significant differences by using two-sample t-test at 0.05 significance level as shown in Fig. 8. Column 4 and 9 of this figure shows the obtained p-values.

Compared to the TDC group, the ASD group showed altered connectivity in 56 regions (24 regions in both right and left hemisphere) (two-sample t-test, $p < 0.05$), as shown in Fig. 8. We have listed these regions in Table 3. The distribution of these regions is largely in accordance with subcortical, cognitive control, default mode, visual, bilateral limbic and auditory networks. These findings are inline with the literature as discussed next and suggest alterations in large scale dynamic functional brain networks in ASD.

3.3. Comparison with static functional connectivity

We computed sFC using MVRC method, resulting in an $N \times N$ size adjacency matrix for each subject of both the groups. Next, we applied two-sample t-test on each FC value of the adjacency matrix, separately, to observe alteration of static FC across the two groups. This approach allowed the determination of regions where sFC differed between the TDC and ASD groups. Compared to the TDC group, the ASD group showed no significant FC alterations across the two groups (FDR corrected at $p \leq 0.05$).

3.4. Validation of the MVRC method on existing studies

In this section, we validate the use of the advanced MVRC method based adjacency matrices in our framework compared to the correlation based matrices on the existing state-of-the-art method of extracting dynamic brain network states. We first provide a brief overview of this existing approach followed by results obtained with MVRC and CORR based dFC matrices.

Conventionally, dynamic brain networks states are identified using correlation matrices computed in sliding windows (Allen et al., 2014; Shakil et al., 2016; Yao et al., 2016). In this approach, first dFC are estimated using correlation in sliding windows. Next, dFC across windows and subjects are vectorized, yielding a dFC data matrix of size $LS \times C$, where L denotes the number of windows, S denotes the number of subjects, and C denotes the $N \times (N-1)/2$ vectorized connections from $N \times N$ FC matrix. Thereafter, dFC time-courses are clustered through k-means that leads to the decomposition of the estimated dFC (of each time-window) into a smaller set of connectivity states. This produces multiple dynamic brain states as shown in Figs. 9 and 10. Results of these states are depicted with reordered regions according to the underlying networks (refer to Yao et al. (2016)). We computed dwell times of identified states for each individual subject in both the groups and carried out two sample t-test ($p < 0.05$) to statistically compare dwell times of the two groups similar to Yao et al. (2016). For the states identified using MVRC adjacency matrices, we observed dwell times of states 1, 2 and 3 to be statistically different, whereas only two states 1 and 3 are found to be different when extracted using CORR adjacency matrices. Thus, MVRC based adjacency matrices are able to reveal differences between the ASD and TDC groups in a better manner.

On further comparing the statistically different states in Figs. 9 and 10, results with both the methods show altered connectivity in cognitive control (CCN), visual (VN), default mode networks (DMN), and other networks. Pearson correlation based connectivity in Fig. 10 shows enhanced (read colors according to color bar) networks in state 1 in ASD and enhanced networks in state 3 in TDC. On the other hand, MVRC based results show enhanced networks in TDC compared to ASD in both the states 1 and 3.

Further, MVRC based connectivity matrices show enhanced connections largely along the block diagonal connections, while Pearson correlation based adjacency matrices show connectivity in almost the entire 90x90 matrix. Thus, Pearson Correlation based adjacency matrices are showing connectivity across the whole brain that may be misleading. Compared to this, MVRC based results can be interpreted visually with ease because enhanced connections are observed along the block diagonal (refer to Fig. 9).

3.5. Reproducibility analysis

In order to check the reproducibility of results on the subset of dataset, we randomly chose 50% subjects of each group of GU dataset and again utilized NNTF to factorize the corresponding dFC tensor into components. Fig. 11 displays the identified overlapping communities that belong to frontal, occipital, limbic, parietal and temporal part of the brain. For both TDC and ASD groups, dynamic brain networks resemble the networks obtained by choosing all the subjects of the dataset. Thus, we obtained consistent results on both the groups. In order to check the reproducibility of results,

	TDC	ASD	*p(h)*			TDC	ASD	*p(h)*
VN	 C1	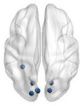 C2	0.9550 (0)		DMN CCN	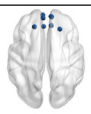 C6	 C1	**1.5507e-04 (1)**
VN	 C2	 C4	0.2128 (0)		SMN AN LN	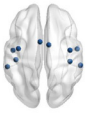 C7	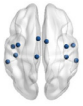 C6	0.59 (0)
AN CCN SCN	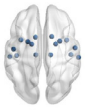 C3	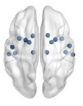 C3	**7.2806e-04 (1)**		BLN	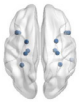 C9	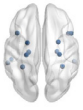 C9	**4.3543e-25 (1)**
VN	 C4	 C5	**0.00048 (1)**		DMN VN	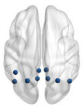 C10	 C10	**8.9224e-16 (1)**
DMN BLN CCN	 C5	 C8	**1.9707e-04 (1)**					

Fig. 8. Results on GU dataset: Statistical difference of strength vectors $\mathbf{s}_r$ of similar networks identied for TDC and ASD groups (refer to Fig. 3). Vectors $\mathbf{s}_r$ are statistically tested using two-sample t-test with 0.05 significance level (column 2). The value of $h = 1$ indicates statistically significant difference in the dFC networks of ASD and control groups ($p < 0.05$). VN: Visual Network; SMN: Somato-Motor Network; AN: Auditory Network; CCN: Cognitive Control Network; DMN: Default Mode Network; SCN: Subcortical Network; LN: Language Network; BLN: Bilateral Limbic Network.

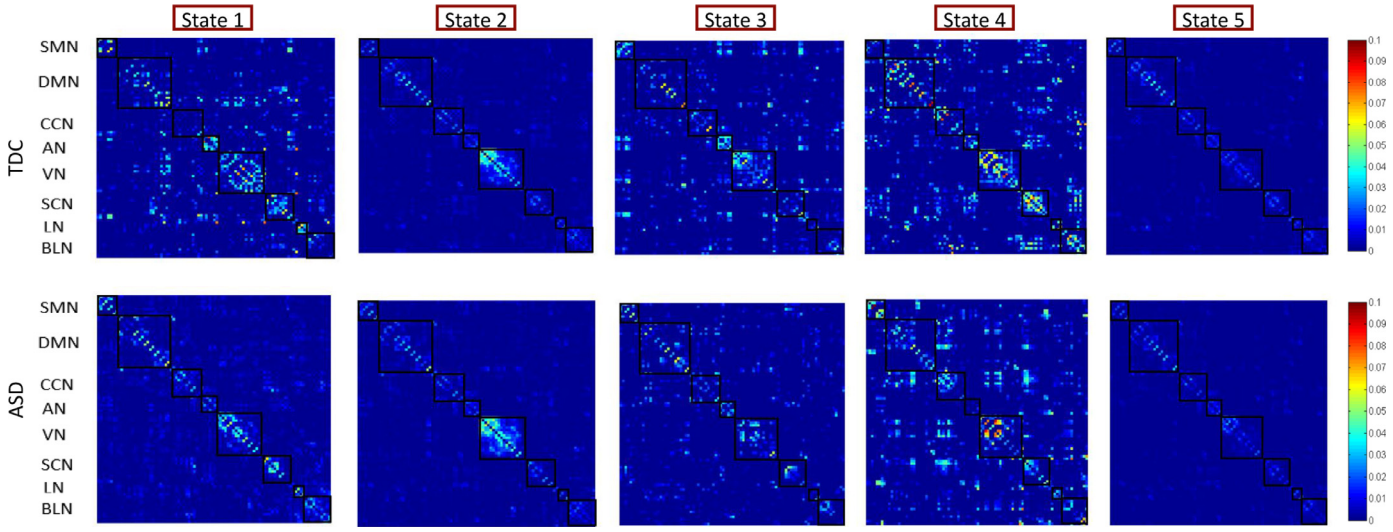

Fig. 9. Results on brain regions' states using the adjacency matrices generated using MVRC.

Table 3
List of altered connectivity regions in Fig. 8.

Network number TDC	Network number ASD	Regions
3	3	RO, INS, CN, PUT, PAL, THA, HG, STG
4	5	CF.R, CUN.L, LG.L, SOG.R
5	8	OSFG.L, OC, MOSFG, GR, TMTG
6	1	DSFG, MSFG, MOSFG.R, ACC
9	9	HIP, PHG, AMY, FG, TSTG, ITG.R
10	10	PCC, SPG.L, AG, PRE

Please refer to Table 2 for abbreviation..L and.R above represent left and right part of the brain.

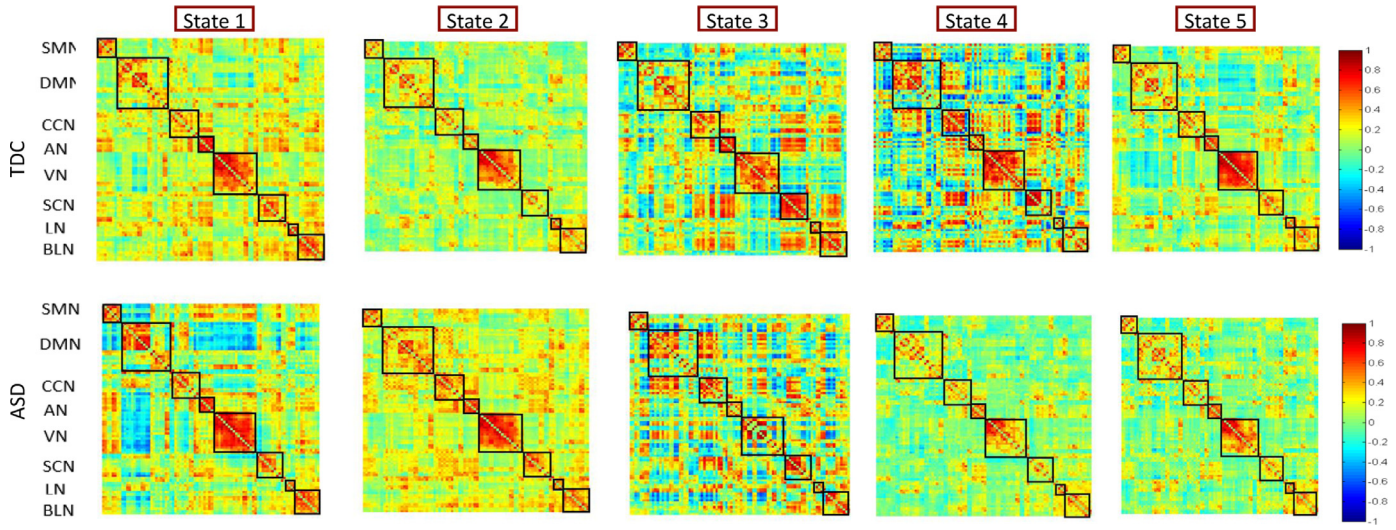

Fig. 10. Results on brain regions' states using the adjacency matrices generated using Pearson correlation.

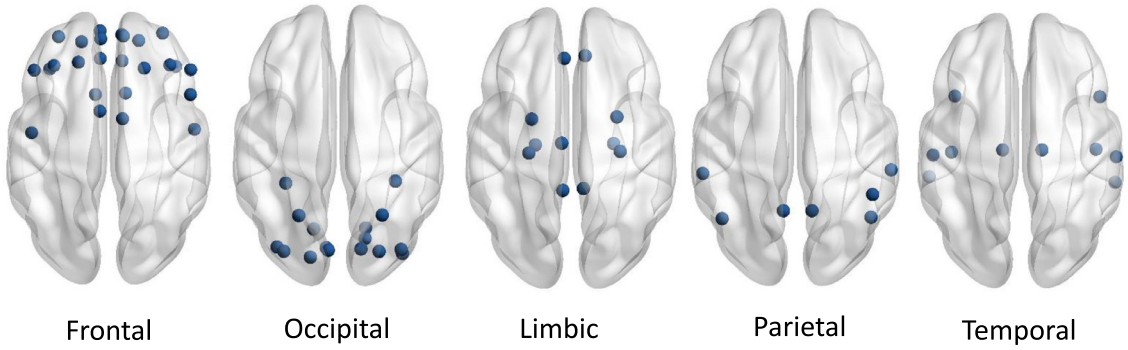

Fig. 11. Group-level dFC networks identified on 50% of the randomly selected subjects of TDC group from the GU dataset.

the proposed method has also been tested on Kennedy Krieger Institute (KKI) ABIDE II dataset[4] (155 normal and 56 autism subjects). Communities obtained from both TDC and ASD groups are shown in Fig. 12. First and second row of this figure show the communities belonging to frontal, occipital, limbic, parietal and temporal parts of the brain, in both the groups. Different colors in this figure imply different communities. In other words, all nodes of one community are shown with one color. For example, three different colored nodes on first axial brain map in TDC row (refer to Fig. 12) is corresponding to three different communities, all lying in the frontal regions. Similar brain activation has been observed in this dataset as was obtained with the GU dataset. In addition, we also tested the strengths of communities between the two groups. We identified a number of altered communities in ASD compared to TDC as shown in the third row of Fig. 12.

4. Discussion

This paper utilizes resting-state fMRI to find aberrant dynamic brain networks in ASD. Autism is increasingly recognized as a common brain disorder with altered brain networks (Hull et al., 2017). It is a neuro-developmental disorder characterized by impaired social interaction and repetitive behaviors (Cherkassky et al., 2006). Despite the progress in the analysis of altered static brain networks in ASD, information regarding time-varying brain networks in autism is still scarce. To address this gap, we have investigated dynamic brain networks' alteration in ASD subjects. In the literature on sFC in autism (Itahashi et al., 2014), it is stated that the presence of group-specific regions in the hubs of ASD group indicates the alteration of hub organization. In this paper, we have studied altered hubs' organization in dynamic functional connectivity compared to that studied for static functional connectivity in Itahashi et al. (2014).

This work contributes to the literature by proposing a method for extracting dynamic overlapping functional brain networks based on advanced signal processing techniques. So far, study of functional brain networks in ASD versus TDC is limited in three respects:

- on building adjacency matrices that are largely built by Pearson Correlation. Pearson correlation has a limitation of providing spurious high correlations because there may be a case that node A is functionally correlated to node B not because nodes A and B are correlated with each other but because both nodes A and B are correlated to node C. This is also known as triangular fBNs in the literature. In the current work, we have used an advanced method (MVRC method) to compute adjacency matrices. This method considers all nodes simultaneously while computing FC and hence, overcomes spurious connection values that arise due to considering two nodes at a time in the Pearson correlation approach.
- on finding networks that are largely computed using modularity yielding non-overlapping networks, while overlapping networks appear to be intuitively more correct as has been done in this work.

[4] http://fcon_1000.projects.nitrc.org/indi/abide/.

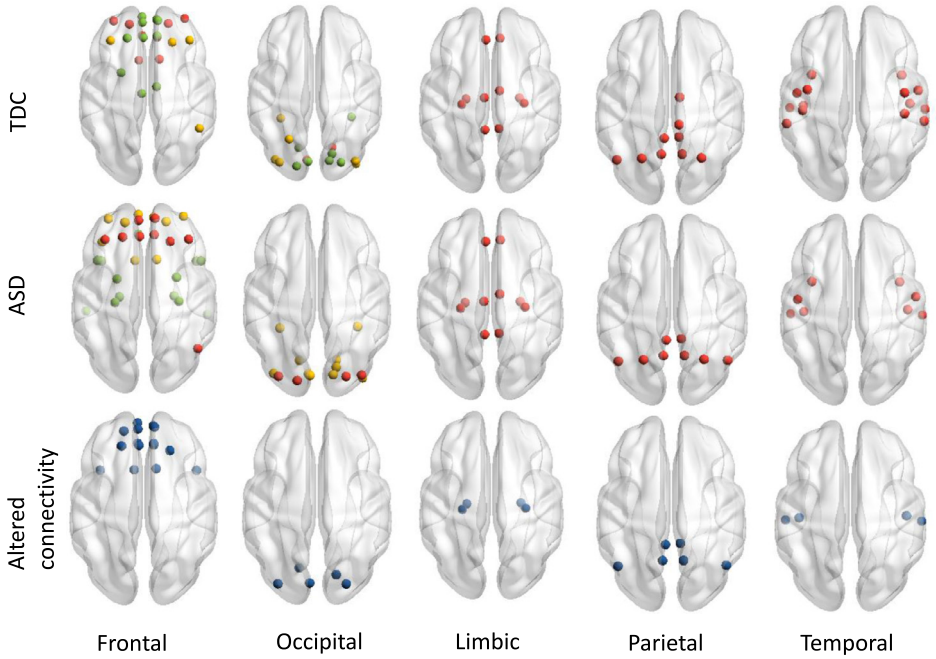

Fig. 12. Dynamic communities obtained on KKI ABIDE dataset. First and second row of this figure show obtained communities, largely lying in the frontal, occipital, limbic, parietal and temporal parts of brain, in both the groups. Third row represents altered communites of both groups ($p < 0.05$).

- in terms of static versus dynamic networks. While extraction of static networks is more common, dynamic networks are more realistic and are being actively worked upon by researchers. The present study expands the current theory of extracting functional brain networks and advocates the use of dynamic analyses to better account for FC differences compared to static FC analysis.

Hence, this study contributes to the literature from the point of view of proposing a novel methodology of extracting dynamic functional brain networks by utilizing multivariate regression based connectivity method along with the extraction of overlapping brain networks.

We analyzed dynamic functional networks, both non-overlapping and overlapping, in ASD vis-à-vis TDC group. Non-overlapping dynamic networks are studied using modularity and alterations were noted in the cognitive control and default mode network. However, these networks could not be identified in all time windows. Most of the windows showed random merging of ROIs belonging to different multiple brain networks. Drastic changes of brain networks indicates less coordination between regions and makes the brain states undifferentiable (Rubenstein and Merzenich, 2003; Uddin et al., 2015).

In addition, 'connector' and 'provincial' hubs were studied based on the level of their intra-module connectivity and inter-module connectivity, i.e., their participation in the multiple modules. Connector hubs are high-degree nodes displaying diverse connectivity profile by connecting with different modules, whereas provincial hubs are high-degree nodes that mostly connect to nodes in the same module (Van Den Heuvel and Sporns, 2013). While both the groups shared same provincial hubs, each group showed group-specific connector hubs, indicating changes in hub organization in autism. These findings indicate that the nodes lying in frontal, parietal and limbic part of the brain are altered in the autistic brain and such alteration is characterized by the changes in the hub pattern in autistic subjects. These regions were found to be impaired in subjects with autism in sFC analysis in previous studies (Bookheimer et al., 2008). This work reports alterations in hubs via dFC analysis.

Overlapping networks were identified using PARAFAC tensor decomposition and results show statistically significant differences in multiple functional brain networks. Differences in the functional brain networks of TDC and ASD groups were assessed using two-sample t-test. We considered differences to be significant when $p < 0.05$. Compared to controls, ASD subjects had a number of altered connections, which involved frontal, occipital, limbic, parietal, and temporal regions. Hence, alterations in whole brain functional brain networks were consistent with the literature.

While comparing MVRC method with the conventional correlation based method, we observed that MVRC based connectivity matrices show enhanced connectivity in TDC compared to ASD, while the Pearson correlation based matrices show some enhanced networks in TDC and some in ASD that may lead to mixed findings. MVRC based results are inline with the belief that there is a reduced coordination among brain regions in autism.

4.1. Consistency with the Literature

In our results, ASD showed altered connectivity in visual network (CF.R, CUN.L, LG.L, SOG.R, and SPG.L) and limbic network (FG), where.R and.L represent right and left parts of the brain, respectively. Alteration in CF (that forms the core of visual cortex) and LG has been reported previously in ASD (Chen et al., 2015). CUN region of VN is responsible for the control of visual attention and refreshing information processing in working memory (Makino et al., 2004). Abnormality in SPG region indicates abnormality for face recognition and other social functions (Jones et al., 2010; Yao et al., 2016). Alteration in OSFG.L, MOSFG, DSFG, MSFG, ACC, PCC, AG, and PRE regions were associated with default mode network. Recently, a previous time-varying network study on ABIDE dataset has noted decreased connectivity for PRE and PCC (Yao et al., 2016), while alteration in ACC connectivity is being reported in Assaf et al. (2010) as has been noted by us. In

addition, we have observed reduced ranking of SFG and AG that is in consonance with global hypoconnectivity noted in these regions in autism subjects (Monk et al., 2009). Further, it is noteworthy that our results show one additional DMN network (number 8) in TDC group compared to the ASD group. This network depicts activation in DSFG, OSFG, and OMFG regions. These regions are a part of DMN and known to be active during resting-state. However, ASD group did not show activation in OMFG as observed from Figure-3. Our findings on aberrant activity in DMN regions confirm it's role in ASD.

Our results showed altered connectivity in INS and no activity in OPIFG.R, TIFG, and SMAG regions in ASD subjects. These results are inline with the aberrant activity in cognitive control network in ASD due to restricted, repetitive behavior and indicate loss in inhibitory control function (Yao et al., 2016). In addition, IFG is related to deficit in social language processing and attentional mechanism and is commonly reported altered in ASD (Ha et al., 2015). Our results showed abnormal connectivity linked to auditory network (HG, RO and STG) in ASD, responsible for speech comprehension and auditory processing in humans (Kana et al., 2016). Subcortical network (CN, PUT, and PAL) are observed to be altered in our analysis. In addition, THA region was not observed to be activated in ASD, indicating less activity in the thalamus cortex in the autistic brain (Nair et al., 2015). Our results showed abnormal connectivity in limbic network (OC, GR, TMTG, HIP, PHG, AMY, TSTG, and ITG.R). This network particularly AMY region has been the focus of ASD related studies, given its important role in socio emotional processing (Baron-Cohen et al., 2000). Previous studies also noted aberrant connectivity in PHG.R (Monk et al., 2009), HIP (Cooper et al., 2017) and SMG (Salmi et al., 2013). ITG is known to be the motion area within the visual cortex of the human brain (Orban et al., 2004) and abnormality in these regions suggests aberrant dFC in autistic subjects compared to the age-matched healthy subjects.

We have also shown the validation of the proposed method on two publicly available dataset. In addition to this, we have also shown the validation of MVRC (an advanced method) based adjacency matrices compared to the Pearson correlation based adjacency matrices on the recent network state method by Yao et al. Results show that findings are more consistent with the literature on revealing differences between the ASD and TDC groups with the MVRC based adjacency matrices compared with those extracted with the Pearson correlation. This also provides credence to our work and establishes the need to use advanced signal processing methods. Since autism is a spectral disorder, we believe that our work on extracting dynamic overlapping functional brain networks using advanced methods is complementary to the work on finding network states. Joint analyses of such works can help in finding potential biomarkers to aid in the diagnosis of Autism disorder.

We have proposed an advanced signal processing methods' based pipeline for the extraction of dynamic functional brain networks in autism. We could locate one interesting study by Yao et al. (2016) on finding network states in autism subjects, while accounting for changes across time. As stated earlier, there is a fundamental difference between this proposed study and the study by Yao et al. (2016) because Yao et al. (2016) studied network states from correlation matrices. They did not extract overlapping dynamic brain networks, while we have presented a method for extracting *overlapping* dynamic brain networks using an advanced multivariate regression method to build FC matrix. Thus, we believe that the proposed work adds information that is complimentary to that obtained with the network state model. Joint analyses of the two methods, both at the group level and at the subject level, can together aid in better understanding of the functioning of brain in ASD.

4.2. Limitations and future directions

Our study in this paper has several limitations. First, although we have extracted dynamic brain networks at the group-level, subject level network analysis is equally important to better understand the relative similarities and differences in the dynamic brain networks of healthy individuals and clinical population. There is a separate concern whether the ABIDE dataset has sufficient power at the individual subject level to identify altered connectivity. Since autism is a spectral disorder and ground truth is never known in real fMRI data, it requires a deeper exploration and rigorous analysis. We intend to handle this concern in the near future with more analyses at the subject level.

Second, the length of the resting state fMRI acquisition in this study is 5 min, although a recent study suggested that dynamic FC analysis should be performed with rs-fMRI acquisitions of greater than 10 min (Hindriks et al., 2016). Since the ground truth is not known in real fMRI data, appropriate duration of data and the length of window are still open questions. Thus, we would suggest a future research on carrying out a thorough investigation of connectivity results obtained with conventional and advanced methods using different statistical analyses on longer duration fMRI dataset, on multi-session data, on data from multiple sources, and on data with varying window lengths.

Third, although we observed altered brain networks across TDC and ASD groups and the observed effects were consistent across a range of analyses, study of dynamic brain networks in ASD is quite challenging owing to it being a disorder over wider spectrum (varying degree of autism across subjects). Further investigation on time-varying abnormalities in these networks will improve the comprehensive understanding of aberrant dFC in ASD. In addition, researchers can also focus on the problem of neuro-rehabilitation, i.e., to devise some intervention techniques that can improve coordination between brain regions. If yes, perhaps these may lead to improved networks with reference to stronger connectivity within a network, reduced overlap across dissimilar networks and lesser differences between TDC vis-à-vis ASD. Both these problems of diagnosis and neuro-rehabilitation are potential research directions.

Fourth, change in window size would definitely introduce change in brain networks. To avoid an arbitrary choice of window length, we considered a lower limit to safely avoid artifacts (Leonardi and Ville, 2015). Changes in window length may introduce possible confounding artifacts. Hence, this question requires a deeper exploration and rigorous analysis. Therefore, we suggest a thorough investigation on the choice of window length as a future research problem.

Fifth, this study includes only male subjects because autism is significantly more common in males than in females. Since the disorder seems to appear more often in male subjects, most of the studies in ASD have studied male subjects. Thus, it is difficult for us to corroborate our findings with the literature on TDC versus ASD in females.

Further, we would like to emphasize that the female data samples are less in most dataset. For example, we have used two widely used public dataset of GU and KKI and both these dataset have a few females subjects. Since we have proposed newer methods and would like to validate it across dataset, we controlled for gender in our study. A group of researchers have recently launched studies on autism in females (Alaerts et al., 2016; Irimia et al., 2017). Investigation of altered brain networks of males versus females in autism is an important research topic. But it requires elaborate research in collaboration with clinicians and neuro-cognitive experts.

Finally, although sliding window approach of dynamic brain networks analysis has gained impetus in fMRI in the neuroscience community (Hutchison et al., 2013a; Allen et al., 2014), work is

needed toward detecting connectivity at each time point. This approach might further provide better understanding of brain network configuration.

5. Conclusions

This study investigated alterations in functional brain networks in subjects with Autistic Spectrum Disorder (ASD) in comparison with Typically Developing Control (TDC) using fMRI data. This research proposed a new framework to detect dynamic brain networks that can be divided into two steps: (1) extraction of dynamic functional connectivity based on the recently proposed MVRC method and the sliding window approach; and (2) usage of a three-mode subject-summarized spatio-temporal tensor to determine overlapping dynamic brain networks and their temporal profiles at the group-level. Statistical significance of aberrant connectivity was observed between ASD and TDC groups on two publicly available resting-state fMRI datasets. We found that the ASD had different functional brain networks from TDC in multiple areas ranging from cognitive control to visual and default mode networks. These findings are inline with the literature and suggest alterations of large-scale brain networks in ASD. Proposed method could detect alterations in functional brain networks in ASD and perhaps, can help in finding biomarkers for human brain disorders. This study demonstrates the potential of using new image analysis strategies to characterize the change in dynamic brain networks in human brain disorders. With further validation, this may become an alternative approach for characterizing diseased state and may possibly have clinical significance in diagnosis and monitoring of neuro-disorders.

Declaration of Competing Interest

None of the authors have any conflicts of interest to declare.

Acknowledgments

The first author would like to thank Visvesvaraya research fellowship, Department of Electronics and Information Tech., Ministry of Comm. and IT (PhD-MIA/4(31)/2014), Govt. of India, for providing financial support for this work. We would also like to thank anonymous reviewers for their useful comments that helped us in improving the quality of this research work.

References

Aarti, N., L., K.C., Michael, D., Patricia, S., Brandon, K., Ralph-Axel, M., 2014. Impact of methodological variables on functional connectivity findings in autism spectrum disorders. Hum. Brain Mapp. 35 (8), 4035–4048. doi:10.1002/hbm.22456.

Aggarwal, P., Gupta, A., 2018. Low rank and sparsity constrained method for identifying overlapping functional brain networks. PLoS ONE 13 (11). doi:10.1371/journal.pone.0208068.

Aggarwal, P., Gupta, A., Garg, A., 2017. Multivariate brain network graph identification in functional MRI. Med. Image Anal. 42, 228–240. doi:10.1016/j.media.2017.08.007.

Alaerts, K., Swinnen, S.P., Wenderoth, N., 2016. Sex differences in autism: a resting-state fmri investigation of functional brain connectivity in males and females. Social Cognit. Affect. Neurosci. 11 (6), 1002–1016. doi:10.1093/scan/nsw027.

Allen, E.A., Damaraju, E., Plis, S.M., Erhardt, E.B., Eichele, T., Calhoun, V.D., 2014. Tracking whole-brain connectivity dynamics in the resting state. Cereb. Cortex 24 (3), 663–676. doi:10.1093/cercor/bhs352.

Assaf, M., Jagannathan, K., Calhoun, V.D., Miller, L., Stevens, M.C., Sahl, R., O'Boyle, J.G., Schultz, R.T., Pearlson, G.D., 2010. Abnormal functional connectivity of default mode sub-networks in autism spectrum disorder patients. NeuroImage 53 (1), 247–256.

Baron-Cohen, S., Ring, H., Bullmore, E., Wheelwright, S., Ashwin, C., Williams, S., 2000. The amygdala theory of autism. Neurosci. Biobehav. Rev. 24 (3), 355–364. doi:10.1016/S0149-7634(00)00011-7.

Benjamini, Y., Hochberg, Y., 1995. Controlling the false discovery rate: a practical and powerful approach to multiple testing. J.R.Stat.Soc. Ser. B (Methodological) 57, 289–300. doi:10.2307/2346101.

Bookheimer, S.Y., Wang, A.T., Scott, A., Sigman, M., Dapretto, M., 2008. Frontal contributions to face processing differences in autism: evidence from fmri of inverted face processing. J. Int. Neuropsychol.Soc. 14 (6), 922–932. doi:10.1017/S135561770808140X.

Calhoun, V.D., Adali, T., Pearlson, G.D., Pekar, J., 2001. A method for making group inferences from functional mri data using independent component analysis. Hum. Brain Mapp. 14 (3), 140–151.

Chang, C., Glover, G.H., 2010. Time-frequency dynamics of resting-state brain connectivity measured with fMRI. NeuroImage 50 (1), 81–98. doi:10.1016/j.neuroimage.2009.12.011.

Chen, C.P., Keown, C.L., Jahedi, A., Nair, A., Pflieger, M.E., Bailey, B.A., Mller, R.-A., 2015. Diagnostic classification of intrinsic functional connectivity highlights somatosensory, default mode, and visual regions in autism. NeuroImage 8, 238–245. doi:10.1016/j.nicl.2015.04.002.

Cherkassky, V.L., Kana, R.K., Keller, T.A., Just, M.A., 2006. Functional connectivity in a baseline resting-state network in autism. Neuroreport 17 (16), 1687–1690.

Cooper, R.A., Richter, F.R., Bays, P.M., Plaisted-Grant, K.C., Baron-Cohen, S., Simons, J.S., 2017. Reduced hippocampal functional connectivity during episodic memory retrieval in autism. Cereb. Cortex 27 (2), 888–902. doi:10.1093/cercor/bhw417.

Frith, U., Happ, F., 1999. Theory of mind and self-consciousness: what is it like to be autistic? Mind Lang. 14 (1), 82–89. doi:10.1111/1468-0017.00100.

Gauvin, L., Panisson, A., Cattuto, C., 2014. Detecting the community structure and activity patterns of temporal networks: a non-negative tensor factorization approach. PLoS ONE 9 (1), 1–13. doi:10.1371/journal.pone.0086028.

Guimera, R., Nunes Amaral, L.A., 2005. Functional cartography of complex metabolic networks. Nature 433 (7028), 895–900. doi:10.1038/nature03288.

Ha, S., Sohn, I.-J., Kim, N., Sim, H.J., Cheon, K.-A., 2015. Characteristics of brains in autism spectrum disorder: structure, function and connectivity across the lifespan. Exp. Neurobiol. 24 (4), 273–284.

Hindriks, R., Adhikari, M., Murayama, Y., Ganzetti, M., Mantini, D., Logothetis, N., Deco, G., 2016. Can sliding-window correlations reveal dynamic functional connectivity in resting-state fMRI? NeuroImage 127, 242–256. doi:10.1016/j.neuroimage.2015.11.055.

Hull, J.V., Jacokes, Z.J., Torgerson, C.M., Irimia, A., Van Horn, J.D., 2017. Resting-state functional connectivity in autism spectrum disorders: a review. Front. Psychiatry 7, 205.

Hutchison, R., Womelsdorf, T., Gati, J., Everling, S., R, S.M., 2013. Resting-state networks show dynamic functional connectivity in awake humans and anesthetized macaques. Hum. Brain Mapp. 2154–2177.

Hutchison, R.M., Womelsdorf, T., Allen, E.A., Bandettini, P.A., Calhoun, V.D., Corbetta, M., Penna, S.D., Duyn, J.H., Glover, G.H., Gonzalez-Castillo, J., Handwerker, D.A., Keilholz, S., Kiviniemi, V., Leopold, D.A., de Pasquale, F., Sporns, O., Walter, M., Chang, C., 2013. Dynamic functional connectivity: promise, issues, and interpretations. NeuroImage 80, 360–378 Mapping the Connectome. doi:10.1016/j.neuroimage.2013.05.079.

Irimia, A., Torgerson, C.M., Jacokes, Z.J., Van Horn, J.D., 2017. The connectomes of males and females with autism spectrum disorder have significantly different white matter connectivity densities. Sci. Rep. 7, 46401.

Itahashi, T., Yamada, T., Watanabe, H., Nakamura, M., Jimbo, D., Shioda, S., Torizuka, K., Kato, N., Hashimoto, R., 2014. Altered network topologies and hub organization in adults with autism: a resting-state fmri study. PLoS ONE 9 (4), 1–15. doi:10.1371/journal.pone.0094115.

Jones, T.B., Bandettini, P.A., Kenworthy, L., Case, L.K., Milleville, S.C., Martin, A., Birn, R.M., 2010. Sources of group differences in functional connectivity: an investigation applied to autism spectrum disorder. NeuroImage 49 (1), 401–414. doi:10.1016/j.neuroimage.2009.07.051.

Kana, R.K., Patriquin, M.A., Black, B.S., Channell, M.M., Wicker, B., 2016. Altered medial frontal and superior temporal response to implicit processing of emotions in autism. Autism Res. 9 (1), 55–66. doi:10.1002/aur.1496.

Karahanolu, F.I., Caballero-Gaudes, C., Lazeyras, F., Ville, D.V.D., 2013. Total activation: fMRI deconvolution through spatio-temporal regularization. NeuroImage 73, 121–134. doi:10.1016/j.neuroimage.2013.01.067.

Kolda, T.G., Bader, B.W., 2009. Tensor decompositions and applications. SIAM Rev. 51 (3), 455–500. doi:10.1137/07070111X.

Lathauwer, L.D., Moor, B.D., Vandewalle, J., 2000. A multilinear singular value decomposition. SIAM J. Matrix Anal. Appl. 21 (4), 1253–1278.

Leonardi, N., Ville, D.V.D., 2015. On spurious and real fluctuations of dynamic functional connectivity during rest. NeuroImage 104, 430–436.

Mahyari, A.G., Zoltowski, D.M., Bernat, E.M., Aviyente, S., 2017. A tensor decomposition-based approach for detecting dynamic network states from eeg. IEEE Trans. Biomed. Eng. 64 (1), 225–237.

Makino, Y., Yokosawa, K., Takeda, Y., Kumada, T., 2004. Visual search and memory search engage extensive overlapping cerebral cortices: an fmri study. NeuroImage 23 (2), 525–533. doi:10.1016/j.neuroimage.2004.06.026.

Minshew, N.J., Keller, T.A., 2010. The nature of brain dysfunction in autism: functional brain imaging studies. Curr. Opin. Neurol. 23 (2), 124.

Monk, C.S., Peltier, S.J., Wiggins, J.L., Weng, S.-J., Carrasco, M., Risi, S., Lord, C., 2009. Abnormalities of intrinsic functional connectivity in autism spectrum disorders. NeuroImage 47 (2), 764–772. doi:10.1016/j.neuroimage.2009.04.069.

Nair, A., Carper, R.A., Abbott, A.E., Chen, C.P., Solders, S., Nakutin, S., Datko, M.C., Fishman, I., Mller, R.-A., 2015. Regional specificity of aberrant thalamocortical connectivity in autism. Hum. Brain Mapp. 36 (11), 4497–4511. doi:10.1002/hbm.22938.

Najafi, M., McMenamin, B.W., Simon, J.Z., Pessoa, L., 2016. Overlapping communities reveal rich structure in large-scale brain networks during rest and task conditions. NeuroImage 135, 92–106. doi:10.1016/j.neuroimage.2016.04.054.

Newman, M.E.J., 2006. Modularity and community structure in networks. Proc. Natl. Acad. Sci. USA 103 (23), 8577–8582.

Newman, M.E.J., Girvan, M., 2004. Finding and evaluating community structure in networks. Phys. Rev. E 69 (2), 026113. doi:10.1103/PhysRevE.69.026113.

Ogawa, S., Lee, T.M., Kay, A.R., Tank, D.W., 1990. Brain magnetic resonance imaging with contrast dependent on blood oxygenation.. Proc. Natl. Acad. Sci. USA 87 (24), 9868–9872.

Orban, G.A., Essen, D.V., Vanduffel, W., 2004. Comparative mapping of higher visual areas in monkeys and humans. Trends Cognit. Sci. 8 (7), 315–324. doi:10.1016/j.tics.2004.05.009.

Ponce-Alvarez, A., Deco, G., Hagmann, P., Romani, G.L., Mantini, D., Corbetta, M., 2015. Resting-state temporal synchronization networks emerge from connectivity topology and heterogeneity. PLoS Comput. Biol. 11 (2), 1–23. doi:10.1371/journal.pcbi.1004100.

Power, J.D., Mitra, A., Laumann, T.O., Snyder, A.Z., Schlaggar, B.L., Petersen, S.E., 2014. Methods to detect, characterize, and remove motion artifact in resting state fMRI. NeuroImage 84, 320–341. doi:10.1016/j.neuroimage.2013.08.048.

Robinson, L.F., Atlas, L.Y., Wager, T.D., 2015. Dynamic functional connectivity using state-based dynamic community structure: method and application to opioid analgesia. NeuroImage 108, 274–291.

Rubenstein, J.L.R., Merzenich, M.M., 2003. Model of autism: increased ratio of excitation/inhibition in key neural systems. Genes Brain Behav. 2 (5), 255–267. doi:10.1034/j.1601-183X.2003.00037.x.

Rubinov, M., Sporns, O., 2010. Complex network measures of brain connectivity: uses and interpretations. NeuroImage 52 (3), 1059–1069. doi:10.1016/j.neuroimage.2009.10.003.

Salmi, J., Roine, U., Glerean, E., Lahnakoski, J., von Wendt, T.N., Tani, P., Leppmki, S., Nummenmaa, L., Jskelinen, I., Carlson, S., Rintahaka, P., Sams, M., 2013. The brains of high functioning autistic individuals do not synchronize with those of others. NeuroImage 3, 489–497. doi:10.1016/j.nicl.2013.10.011.

Shakil, S., Lee, C.-H., Keilholz, S.D., 2016. Evaluation of sliding window correlation performance for characterizing dynamic functional connectivity and brain states. NeuroImage 133, 111–128. doi:10.1016/j.neuroimage.2016.02.074.

Sporns, O., Betzel, R.F., 2016. Modular brain networks. Annu. Rev. Psychol. 67, 613–640.

Thompson, W.H., Fransson, P., 2015. The frequency dimension of fMRI dynamic connectivity: network connectivity, functional hubs and integration in the resting brain. NeuroImage 121, 227–242.

Tzourio-Mazoyer, N., Landeau, B., Papathanassiou, D., Crivello, F., Etard, O., Delcroix, N., Mazoyer, B., Joliot, M., 2002. Automated anatomical labeling of activations in SPM using a macroscopic anatomical parcellation of the MNI MRI single-subject brain. NeuroImage 15 (1), 273–289. doi:10.1006/nimg.2001.0978.

Uddin, L.Q., Supekar, K., Lynch, C.J., Cheng, K.M., Odriozola, P., Barth, M.E., Phillips, J., Feinstein, C., Abrams, D.A., Menon, V., 2015. Brain state differentiation and behavioral inflexibility in autism. Cereb. Cortex 25 (12), 4740–4747. doi:10.1093/cercor/bhu161.

Van Den Heuvel, M.P., Sporns, O., 2013. Network hubs in the human brain. Trends Cognit. Sci. 17 (12), 683–696.

Wiggins, J.L., Peltier, S.J., Ashinoff, S., Weng, S.-J., Carrasco, M., Welsh, R.C., Lord, C., Monk, C.S., 2011. Using a self-organizing map algorithm to detect age-related changes in functional connectivity during rest in autism spectrum disorders. Brain Res. 1380, 187–197. doi:10.1016/j.brainres.2010.10.102. The Emerging Neuroscience of Autism Spectrum Disorders

Yao, Z., Hu, B., Xie, Y., Zheng, F., Liu, G., Chen, X., Zheng, W., 2016. Resting-state time-varying analysis reveals aberrant variations of functional connectivity in autism. Front. Hum. Neurosci. 10, 463. doi:10.3389/fnhum.2016.00463.

Zhang, Q., Wang, Y., Levine, M.D., Yuan, X., Wang, L., 2015. Multisensor video fusion based on higher order singular value decomposition. Inf. Fusion 24, 54–71.